



Published in final edited form as:

J Cell Physiol. 2012 February ; 227(2): 401–407. doi:10.1002/jcp.22955.

Galectin-3 is a new MerTK-specific eat-me signal

Nora B. Caberoy, Gabriela Alvarado, Jo-Lawrence Bigcas, and Wei Li*

Bascom Palmer Eye Institute, Department of Ophthalmology, University of Miami School of Medicine, Miami, FL 33136, USA

Abstract

Phagocytosis of apoptotic cells and cellular debris is a critical process of maintaining tissue and immune homeostasis. Defects in the phagocytosis process cause autoimmunity and degenerative diseases. Phagocytosis ligands or “eat-me” signals control the initiation of the process by linking apoptotic cells to receptors on phagocyte surface and triggering signaling cascades for cargo engulfment. Eat-me signals are traditionally identified on a case-by-case basis with challenges, and the identification of their cognate receptors is equally daunting. Here we identified galectin-3 (Gal-3) as a new MerTK ligand by an advanced dual functional cloning strategy, in which phagocytosis-based functional cloning is combined with receptor-based affinity cloning to directly identify receptor-specific eat-me signal. Gal-3 interaction with MerTK was independently verified by co-immunoprecipitation. Functional analyses showed that Gal-3 stimulates the phagocytosis of apoptotic cells and cellular debris by macrophages and retinal pigment epithelial cells with MerTK activation and autophosphorylation. The Gal-3-mediated phagocytosis was blocked by excessive soluble MerTK extracellular domain and lactose. These results suggest that Gal-3 is a legitimate MerTK-specific eat-me signal. The strategy of dual functional cloning with applicability to other phagocytic receptors will facilitate unbiased identification of their unknown ligands and improve our capacity for therapeutic modulation of phagocytic activity and innate immune response.

Keywords

Galectin-3; MerTK; Phagocytosis; Eat-me signal; Phagocytosis ligand; Retinal pigment epithelium cell; Macrophage; ORF phage display

Phagocytic clearance of apoptotic cells and cellular debris is critical for the maintenance of tissue and immune homeostasis (Erwig and Henson, 2007; Ravichandran and Lorenz, 2007). Abnormal phagocytosis has been implicated in an array of diseases, including autoimmunity, retinal degeneration, atherosclerosis, tumor evasion from immune surveillance and infectious diseases (Erwig and Henson, 2007; Strick and Vollrath, 2010; Thorp and Tabas, 2009). Phagocytosis ligands or “eat-me” signals control the initiation of the process and hold the key to molecular insights of phagocyte biology with therapeutic potentials to regulate phagocytosis activity under physiological and pathological conditions. The critical barrier to unraveling the molecular mystery of phagocytosis biology is how to identify unknown phagocytosis ligands, cognate receptors and signaling cascades. Nearly all known phagocytosis ligands, including receptor-specific ligands, have been identified on a case-by-case basis with daunting challenges.

Mer receptor tyrosine kinase (MerTK) is one of the well-characterized phagocytic receptors. Mutations of MerTK cause defect in phagocytosis, leading to accumulation of

*Corresponding author: Wei Li, Ph.D., Bascom Palmer Eye Institute, Department of Ophthalmology, University of Miami School of Medicine, Miami, FL 33136, USA. Tel: +1-305-326-6445, Fax: +1-305-547-3658, wli@med.miami.edu.

unphagocytosed debris, retinal degeneration, autoimmunity and atherosclerosis (Kevany and Palczewski, 2010; Rothlin and Lemke, 2010; Thorp and Tabas, 2009). Gas6 and protein S were identified as MerTK ligands more than 15 years ago (Nagata et al., 1996). We recently developed open reading frame (ORF) phage display as a new technology of functional proteomics (Li and Caberoy, 2010) and identified tubby and tubby-like protein 1 (Tulp1) as new MerTK ligands by a unique cloning strategy of phagocytosis-based functional selection (Caberoy et al., 2010a; Caberoy et al., 2010c). These results suggested that MerTK is a phagocytic receptor with multiple ligands.

Here we describe a dual functional cloning strategy which combines phagocytosis-based functional selection with receptor-based affinity selection for unbiased identification of receptor-specific eat-me signals. We identified galectin-3 (Gal-3) as a new MerTK-specific ligand and independently validated the protein with multiple lines of evidence, including its functional activity, co-immunoprecipitation, receptor activation and functional blockade with the receptor extracellular domain. These results demonstrated the validity of the dual functional selection of ORF phage display to identify receptor-specific phagocytosis ligands. The implications of these findings in molecular phagocyte biology, retinal degeneration, tumor immune surveillance and tissue aging are discussed.

Materials and Methods

Dual phage selections

An ORF phage display cDNA library of mouse eye was described previously (Caberoy et al., 2010b). Phagocytosis-based functional selection was carried out in D407 retinal pigment epithelial (RPE) cells with $\sim 1 \times 10^{11}$ pfu (plaque forming unit) of library phages as described (Caberoy et al., 2010a; Caberoy et al., 2009b). Briefly, phage library was amplified in BLT5615 bacteria, precipitated with polyethylene glycol-8000, resuspended in the culture medium, quantified by plaque assay, incubated with D407 RPE cells in 35-mm culture dishes for 30 min at 4°C without phagocytosis. After washing, the cells with bound phages were incubated at 37°C for 30 min for phagocytosis. Unphagocytosed surface-bound phages were stripped off by incubating the cells in the stripping buffer (100 mM glycine, pH 2.5, 150 mM NaCl, 200 mM urea, 2 mg/ml polyvinylpyrrolidone) for 2 min \times 2 times at room temperature, followed by a quick wash with ice-cold phosphate buffered saline (PBS). Internalized phages were released by the lysis buffer (1 mM triethylamine with 0.5% Triton X-100) for 1 min and immediately neutralized to pH 7.4 with 10X PBS premixed with diluted HCl. Released phages were amplified in BLT5615 bacteria, and used as input for receptor-based phage affinity selection with Mer-Fc (MerTK extracellular domain fused to human IgG1 Fc domain, R&D Systems), as described (Caberoy et al., 2010b). Briefly, Mer-Fc was immobilized on ELISA plates (5 μ g/ml, 100 μ l/well), blocked with 10% polyvinyl alcohol (PVA), and incubated with the enriched phages for 1 h at 4°C. After washing, bound phages were eluted by 3C protease cleavage at 4°C overnight, amplified and used as input for the next round of phagocytosis-based functional selection. Phagocytosed phages and bound phages at each round were quantified by plaque assay. After 4 rounds of combined selections, one round of post-panning selection with immobilized streptavidin was performed to eliminate non-ORF clones. Individual phage clones were randomly picked from phage plates and analyzed for their phagocytosis activity in D407 cells (Caberoy et al., 2010a). Positive clones were further analyzed for their Mer-Fc binding activity (Caberoy et al., 2010b).

Phagocytosis assay

Plasma membrane-targeted green fluorescent protein (mGFP) was expressed in Neuro-2a cells with or without Gal-3 co-expression. mGFP-labeled membrane vesicles were prepared

from the Neuro-2a cells at 48 h post-transfection, used for phagocytosis assay with D407 RPE cells or J774 macrophages, washed and analyzed by confocal microscopy or flow cytometry, as described (Caberoy et al., 2010a). Alternatively, we prepared plasma membrane vesicles from control Neuro-2a cells, labeled the vesicles with CFSE or pHrodo, and used the labeled vesicles for phagocytosis assay in the presence or absence of purified glutathione S-transferase-Gal-3 fusion protein (GST-Gal-3). Fluorescence-labeled membrane vesicles were incubated with D407 or J774 cells for 3 h at 37°C in serum-free 293 SFM II medium (Invitrogen), followed by extensive washing. To distinguish between the phagocytosed and surface-bound cargos by confocal microscopy, we scanned the cells for multiple z-stacks of confocal images, located the z-stack with the highest nuclear staining of DAPI blue signals as cross-section of phagocytes and analyzed the phagocytosed green fluorescence signals on the same z-stack. Relative fluorescence intensity per cell was measured using Leica Application Suite software by manually tracing the outline of individual phagocytes under the cognate bright field channel with the corresponding fluorescence quantified in the GFP/CFSE channel. To distinguish between the phagocytosed and surface-bound cargos by flow cytometry, the phagocytes after phagocytosis were treated with trypsin to remove surface-bound cargos and washed before flow cytometric quantification. All the cells were gated with the forward scatter and side scatter to eliminate possible surface-bound cargos.

Jurkat cells were labeled with CFSE, washed and cultured in the presence or absence of 40 μ M etoposide to induce apoptosis, as described (Caberoy et al., 2010c). After washing, the apoptotic or healthy Jurkat cells were verified by staining with annexin V and propidium iodide, used for macrophage phagocytosis assay in the presence or absence of purified GST-Gal-3, and analyzed by confocal microscopy or flow cytometry. Percentage of macrophages with phagocytosed CFSE-labeled cells were quantified with at least 20 viewing fields per group. GST-Gal-3 was constructed, expressed and purified, as described (Caberoy et al., 2010a).

Co-immunoprecipitation

Neuro-2a cells were transfected with plasmids expressing Gal-3-FLAG or control GFP-FLAG (Caberoy et al., 2010a) using Lipofectamine (Invitrogen), collected at 48 h post-transfection, washed and lysed in PBS with 0.5% Triton X-100. The cell lysates were incubated with Mer-Fc (0.5 μ g) for 1 h at 4°C, followed by protein A-agarose beads. The beads were washed and analyzed by Western blot using anti-FLAG monoclonal antibody (mAb) (Sigma), as described (Caberoy et al., 2010c).

Alternatively, purified GST-Gal-3 fusion protein (1 μ g) was incubated with Mer-Fc (0.5 μ g) in 1 ml of PBS plus 0.2% Tween-20 for 1 h at 4°C, followed by protein A-agarose beads. The beads were washed and analyzed by Western blot using anti-GST mAb (AnaSpec).

MerTK phosphorylation

D407 and J774 cells were cultured in 293 SFM II medium for 2 h to reduce the background of MerTK activation, followed by incubation with purified GST-Gal-3, GST or Gas6 in the same medium for 30 min at 37°C. After washing, the cells were lysed and immunoprecipitated with anti-MerTK antibodies (Abs) (Fabgennix, Frisco, TX) and analyzed by Western blot with anti-phospho-MerTK Ab (Fabgennix, Frisco, TX) or anti-MerTK Ab, as described (Caberoy et al., 2010c).

Data analysis

All experiments were repeated independently at least 3 times. Data were analyzed by Student's t-test or Tukey-Kramer multiple comparisons test using GraphPad InStat software.

Results

Dual functional selection

To identify new MerTK ligands, we developed a dual functional selection system (Fig. 1A). The ORF phage display cDNA library of mouse eyes was enriched by phagocytosis-based functional selection using D407 RPE cells. Phagocytosed phages were released by cell lysis, amplified and re-selected by receptor-binding selection with immobilized Mer-Fc. Four rounds of combined selections resulted in substantial increases in the phagocytosis activity and Mer-Fc-binding activity (Fig. 1B,C).

Individual phage clones were analyzed for their internalization activity in D407 cells (Supplementary Fig. S1). All clones with at least 10-fold increase in phagocytosis activity versus the control phage without cDNA insert were subject to additional phage binding assay with immobilized Mer-Fc (Supplementary Fig. S2). Among 11 identified proteins were Tulp1 (GenBank Accession #NM_021478) and Gal-3 (NM_010705, 131Y-264I). Two independent Tulp1 clones were identified, including 178K-251V and 149P-277V, both of which encoded 2 and 4 minimal phagocytosis domains (MPDs) of K/R(X)₁₋₂KKK, respectively. We recently mapped MPDs as essential MerTK-binding motifs for tubby and Tulp1 (Caberoy et al., 2010c). Our earlier study of phagocytosis-basis functional selection with ARPE19 cells identified Tulp1 (79A-199T) with 2 MPDs (Caberoy et al., 2010a). These results suggested the validity of our dual functional cloning.

Gal-3 facilitates RPE phagocytosis

To independently validate Gal-3 stimulation of RPE phagocytosis, we co-expressed Gal-3 with C-terminal FLAG tag (Gal-3-FLAG) and mGFP in Neuro-2a cells. mGFP-labeled membrane vesicles with average size of $2.07 \pm 0.98 \mu\text{m}$ (\pm s.d.) were prepared from Gal-3-expressing cells or control cells, incubated with D407 RPE cells for phagocytosis and analyzed by confocal microscopy. The results showed that Gal-3 significantly stimulated RPE phagocytosis with ~4-fold increase in the activity (Fig. 2A,B).

In addition, mGFP-labeled membrane vesicles were prepared from control Neuro-2a cells, incubated with RPE cells in the presence or absence of purified GST-Gal-3 and analyzed by flow cytometry. The results showed that Gal-3 at 50 or 200 nM stimulated RPE phagocytosis (Fig. 2C). Excessive lactose reduced Gal-3-mediated RPE phagocytosis, suggesting that the C-terminal carbohydrate binding domain (CBD) of Gal-3 plays an important role in facilitating RPE phagocytosis. Partial reduction of Gal-3-mediated phagocytosis by lactose suggested that Gal-3 may bind to phagocytosis preys not only through lectin-carbohydrate interactions, but also through other protein-protein interactions (Dumic et al., 2006). Dose-dependent blockade of Gal-3-mediated phagocytosis by lactose was showed in Supplementary Fig. S3.

Gal-3 stimulates macrophage phagocytosis

MerTK phagocytosis pathway is highly conserved among different phagocytes (Ravichandran and Lorenz, 2007). To investigate Gal-3 capacity to stimulate phagocytosis of other phagocytes, we incubated fluorescence-labeled healthy or apoptotic Jurkat cells with J774 macrophage cell line in the presence or absence of GST-Gal-3, analyzed and quantified the phagocytosed Jurkat cells by confocal microscopy. The results showed that Gal-3 significantly stimulated macrophage phagocytosis of apoptotic Jurkat cells (~3.5-fold increase in activity, $p < 0.001$), but not the healthy cells (Fig. 3A,B). Phagocytosed apoptotic cells with clearly visible fluorescent signals were detected inside the cell body of macrophages. In addition, we labeled apoptotic or healthy Jurkat cells with pHrodo, a fluorogenic dye with no fluorescence at neutral pH but drastically increases in red

fluorescence in acidic phagosomes (Miksa et al., 2009). Coupled with confocal microscopy, pHrodo reliably distinguished between ingested and uningested cargos (Supplementary Fig. S4).

Macrophage phagocytosis of apoptotic cells was further revealed by flow cytometry. GST-Gal-3 at 50 nM and 200 nM facilitated the phagocytosis of apoptotic Jurkat cells (Fig. 3C). However, Gal-3 at 1,000 nM had a reduced activity, suggesting that Gal-3 stimulates macrophage phagocytosis in a biphasic concentration-dependent manner. Gal-3 at 1,000 nM had no impact on the viability of D407 cells (Supplementary Fig. S5). Similarly, excessive lactose partially blocked macrophage phagocytosis. Membrane vesicles prepared from Gal-3-expressing Neuro-2a cells were further analyzed for macrophage phagocytosis. The results showed that Gal-3-vesicles, but not control vesicles, were preferentially phagocytosed by macrophages (Fig. 3D,E).

Gal-3 as a new MerTK ligand

Gal-3 without a classical signal peptide is one of the well-characterized proteins for its unconventional secretion (Hughes, 1999) and has physiological access to MerTK on phagocyte surface. We validated Gal-3 interaction with MerTK by co-immunoprecipitating Gal-3-FLAG in Neuro-2a cell lysate with Mer-Fc (Fig. 4A). Similar co-immunoprecipitation results were obtained with GST-Gal-3 and Mer-Fc (Fig. 4B).

A protein with binding activity to a receptor may not always be a genuine ligand, unless it is capable of activating the receptor. MerTK activation was characterized by autophosphorylation of intracellular tyrosine residues. Our results showed that Gal-3 induced MerTK autophosphorylation in J774 and D407 cells in a dose-dependent manner (Fig. 4C, Supplementary Fig. S6). These data suggest that Gal-3 is a genuine MerTK ligand.

Gal-3 is a bridging molecule

All four known MerTK ligands, including Gas6, protein S, tubby and Tulp1, function as bridging molecules by simultaneously binding to MerTK and phagocytosis preys through different domains to stimulate phagocytosis (Caberoy et al., 2010c; Ravichandran and Lorenz, 2007). To investigate whether Gal-3 is a bridging molecule, we pre-incubated Gal-3 with mGFP-labeled control membrane vesicles of Neuro-2a cells. After washing, the vesicles were analyzed for D407 RPE phagocytosis in the presence or absence of excessive Mer-Fc. The results showed that soluble Gal-3 bound to the vesicles and stimulated the phagocytosis, which was blocked by excessive Mer-Fc (Fig. 4D,E). Dose-dependent blockade of Gal-3-mediated phagocytosis by Mer-Fc was shown in Supplementary Fig. S7. Taken together, these data suggest that Gal-3 facilitates phagocytosis as MerTK-specific bridging molecule. Reduced RPE phagocytosis at the high concentration of Gal-3 (1,000 nM) (Fig. 3C) may reflect its decreased efficiency to bridge phagocytosis preys to MerTK by the same Gal-3 molecule, similar to the reduced plasmid ligation efficiency with excess DNA inserts. However, Gal-3 direct interaction with MerTK should not be affected by the decreased bridging efficiency at the high concentration (Supplementary Fig. S6).

Discussion

The participation of Gal-3 in phagocytosis was previously reported by several groups but with controversy on its underlying molecular mechanisms. Sano et al. (Sano et al., 2003) demonstrated with Gal-3^{-/-} macrophages that Gal-3 facilitates macrophage phagocytosis through intracellular mechanisms. This conclusion was supported by intracellular Gal-3 to activate phosphatidylinositol-3-kinase (PI3K) via K-Ras to promote microglial phagocytosis (Rotshenker et al., 2008). However, Fernández et al. (Fernandez et al., 2005) showed that

extracellular recombinant Gal-3 stimulated neutrophil phagocytosis through an uncharacterized mechanism and can be blocked by lactose. The controversial intracellular and extracellular mechanisms of Gal-3 in regulating phagocytosis may be reconciled by the fact that Gal-3 has more than four dozens of functions (Dumic et al., 2006). Gal-3 may promote phagocytosis through both intracellular and extracellular mechanisms. The results of this study suggest that extracellular Gal-3 facilitates phagocytosis of apoptotic cells or debris through MerTK receptor.

Gas6 and protein S are two well-characterized MerTK ligands with their C-terminal $2 \times$ LG domains as receptor-binding domains (Hafizi and Dahlback, 2006). Tubby and Tulp1 were recently identified as MerTK ligands by phagocytosis-based functional selection of ORF phage display and mapped with MPDs as the MerTK-binding motifs (Caberoy et al., 2010c). Gal-3 was identified by dual functional cloning with its entire C-terminal domain, suggesting that this domain harbors a MerTK-binding motif with no sequence homology to the $2 \times$ LG domains or MPD motif. The exact MerTK-binding motif of Gal-3 is yet to be determined. In addition, Gal-3 C-terminal CBD binds to glycoproteins as a phagocytosis prey-binding domain (PPBD) (ref). Lactose partially reduced Gal-3 capacity to stimulate phagocytosis (Fig. 2C, 3C), suggesting that Gal-3 is the first bridging molecule with binding activity to glycoproteins. Gal-3 and tubby have moderate additive effect to facilitate macrophage phagocytosis of apoptotic cells (Supplementary Fig. S8).

The finding of Gal-3 as an eat-me signal to facilitate MerTK-mediated phagocytosis has several physiological and pathological implications. An earlier study showed that constant light exposure not only induced photoreceptor degeneration, but also upregulated Gal-3 expression in retinal Muller cells (Uehara et al., 2001). The light-induced Gal-3 can be released via its unconventional secretion (Hughes, 1999) or from the damaged retina to facilitate the clearance of damaged photoreceptor outer segments by the RPE to maintain retinal homeostasis as an eat-me signal. Moreover, Gal-3 is a well-characterized binding protein for advanced glycation end products (AGEs) (Vlassara et al., 1995), which have been implicated in tissue aging, including retinal aging, diabetes and Alzheimer's disease (Barile and Schmidt, 2007; Grillo and Colombatto, 2008). Gal-3 plays an important role in the clearance of AGEs to prevent age-related tissue damage through undefined mechanisms (Iacobini et al., 2005). Our results implicate that Gal-3 may facilitate AGE clearance through MerTK-mediated phagocytosis. In addition, Gal-3 is a tumor biomarker with increased expression in invasive tumors (Canesin et al., 2010). MerTK-mediated phagocytosis is well known for immunosuppression and immune tolerance (Rothlin and Lemke, 2010). In this regard, Gal-3 as a MerTK ligand may contribute to tumor evasion from immune surveillance.

ORF phage display is a key for the dual functional cloning. Because of uncontrollable reading frames, the majority of phage clones (~90–94%) identified from conventional cDNA libraries are non-ORFs encoding unnatural short peptides with minimal implication in cellular protein interaction networks (Li and Caberoy, 2010). We developed a new system of ORF phage display with minimal reading frame problem (Caberoy et al., 2010b). Our T7 phage-based ORF display system without requiring the displayed proteins to be secreted through *E. coli* membrane, as required in filamentous phage (Paschke, 2006), is particularly suitable for unbiased display of mammalian proteins (Bratkovic, 2010; Krumpke et al., 2006). We proposed for the first time that ORF phage display can be used as a new technology of functional proteomics, and demonstrated its four versatile applications, including phagocytosis-based functional selection and protein-based affinity selection (Caberoy et al., 2010a; Caberoy et al., 2009a; Caberoy et al., 2010b; Kim et al., 2011).

This study identified Gal-3 as a novel MerTK ligand by an innovative dual functional cloning technique, whose validity was demonstrated by the identification of Tulp1 as a known MerTK ligand and the characterization of Gal-3. The daunting challenge to unravel the mystery of molecular phagocyte biology is how to identify unknown signaling pathways in the absence of any molecular probe. The unique phagocytosis-based functional selection is the only available technology for unbiased identification of eat-me signals in the absence of receptor information and is applicable to various professional and non-professional phagocytes (Caberoy et al., 2010a; Caberoy et al., 2009b). Identified ligands can be used as molecular probes to identify cognate phagocytic receptors and intracellular signaling cascades (Caberoy et al., 2010c). The dual functional cloning described in this study will further advance our capacity to map receptor-specific phagocytosis ligands for comprehensive understanding of molecular phagocyte biology. This approach is applicable to many other phagocytic receptors with unknown ligands, including triggering receptors expressed by myeloid cells-2 (TREM2) and signal-regulatory protein- β 1 (SIRP β 1) that are important to regulate innate immune response and prevent neurodegeneration (Hsieh et al., 2009; Neumann and Takahashi, 2007). Therefore, both approaches will provide in-depth understanding of the physiological and pathological roles of various phagocytes and improve our capability to modulate phagocytosis activity for disease therapy.

Supplementary Material

Refer to Web version on PubMed Central for supplementary material.

Acknowledgments

We thank G. Gaidosh at the confocal core facility of the Bascom Palmer Eye Institute. This project was partially supported by NIH R01EY016211, R01EY016211-05S1, P30-EY014801 and an institutional grant from Research to Prevent Blindness.

Literature Cited

- Barile GR, Schmidt AM. RAGE and its ligands in retinal disease. *Curr Mol Med*. 2007; 7(8):758–765. [PubMed: 18331234]
- Bratkovic T. Progress in phage display: evolution of the technique and its application. *Cell Mol Life Sci*. 2010; 67(5):749–767. [PubMed: 20196239]
- Caberoy NB, Maignel D, Kim Y, Li W. Identification of tubby and tubby-like protein 1 as eat-me signals by phage display. *Exp Cell Res*. 2010a; 316(2):245–257. [PubMed: 19837063]
- Caberoy NB, Zhou Y, Alvarado G, Fan X, Li W. Efficient identification of phosphatidylserine-binding proteins by ORF phage display. *Biochem Biophys Res Commun*. 2009a; 386(1):197–201. [PubMed: 19520055]
- Caberoy NB, Zhou Y, Jiang X, Alvarado G, Li W. Efficient identification of tubby-binding proteins by an improved system of T7 phage display. *J Mol Recognit*. 2010b; 23(1):74–83. [PubMed: 19718693]
- Caberoy NB, Zhou Y, Li W. Can phage display be used as a tool to functionally identify endogenous eat-me signals in phagocytosis? *J Biomol Screen*. 2009b; 14(6):653–661. [PubMed: 19531662]
- Caberoy NB, Zhou Y, Li W. Tubby and tubby-like protein 1 are new MerTK ligands for phagocytosis. *EMBO J*. 2010c; 29(23):3898–3910. [PubMed: 20978472]
- Canesin G, Gonzalez-Peramato P, Palou J, Urrutia M, Cordon-Cardo C, Sanchez-Carbayo M. Galectin-3 expression is associated with bladder cancer progression and clinical outcome. *Tumour Biol*. 2010; 31(4):277–285. [PubMed: 20401558]
- Dumic J, Dabelic S, Flogel M. Galectin-3: an open-ended story. *Biochim Biophys Acta*. 2006; 1760(4):616–635. [PubMed: 16478649]
- Erwig LP, Henson PM. Immunological consequences of apoptotic cell phagocytosis. *Am J Pathol*. 2007; 171(1):2–8. [PubMed: 17591947]

- Fernandez GC, Ilarregui JM, Rubel CJ, Toscano MA, Gomez SA, Beigier Bompadre M, Isturiz MA, Rabinovich GA, Palermo MS. Galectin-3 and soluble fibrinogen act in concert to modulate neutrophil activation and survival: involvement of alternative MAPK pathways. *Glycobiology*. 2005; 15(5):519–527. [PubMed: 15604089]
- Grillo MA, Colombatto S. Advanced glycation end-products (AGEs): involvement in aging and in neurodegenerative diseases. *Amino Acids*. 2008; 35(1):29–36. [PubMed: 18008028]
- Hafizi S, Dahlback B. Gas6 and protein S. Vitamin K-dependent ligands for the Axl receptor tyrosine kinase subfamily. *Febs J*. 2006; 273(23):5231–5244. [PubMed: 17064312]
- Hsieh CL, Koike M, Spusta SC, Niemi EC, Yenari M, Nakamura MC, Seaman WE. A role for TREM2 ligands in the phagocytosis of apoptotic neuronal cells by microglia. *J Neurochem*. 2009; 109(4):1144–1156. [PubMed: 19302484]
- Hughes RC. Secretion of the galectin family of mammalian carbohydrate-binding proteins. *Biochim Biophys Acta*. 1999; 1473(1):172–185. [PubMed: 10580137]
- Iacobini C, Oddi G, Menini S, Amadio L, Ricci C, Di Pippo C, Sorcini M, Pricci F, Pugliese F, Pugliese G. Development of age-dependent glomerular lesions in galectin-3/AGE-receptor-3 knockout mice. *Am J Physiol Renal Physiol*. 2005; 289(3):F611–F621. [PubMed: 15870382]
- Kevany BM, Palczewski K. Phagocytosis of retinal rod and cone photoreceptors. *Physiology (Bethesda)*. 2010; 25(1):8–15. [PubMed: 20134024]
- Kim Y, Caberoy NB, Alvarado G, Davis JL, Feuer WJ, Li W. Identification of Hnrph3 as an autoantigen for acute anterior uveitis. *Clin Immunol*. 2011; 138(1):60–66. [PubMed: 20943442]
- Krumpe LR, Atkinson AJ, Smythers GW, Kandel A, Schumacher KM, McMahon JB, Makowski L, Mori T. T7 lytic phage-displayed peptide libraries exhibit less sequence bias than M13 filamentous phage-displayed peptide libraries. *Proteomics*. 2006; 6(15):4210–4222. [PubMed: 16819727]
- Li W, Caberoy NB. New perspective for phage display as an efficient and versatile technology of functional proteomics. *Appl Microbiol Biotechnol*. 2010; 85(4):909–919. [PubMed: 19885657]
- Miksa M, Komura H, Wu R, Shah KG, Wang P. A novel method to determine the engulfment of apoptotic cells by macrophages using pHrodo succinimidyl ester. *J Immunol Methods*. 2009; 342(1–2):71–77. [PubMed: 19135446]
- Nagata K, Ohashi K, Nakano T, Arita H, Zong C, Hanafusa H, Mizuno K. Identification of the product of growth arrest-specific gene 6 as a common ligand for Axl, Sky, and Mer receptor tyrosine kinases. *J Biol Chem*. 1996; 271(47):30022–30027. [PubMed: 8939948]
- Neumann H, Takahashi K. Essential role of the microglial triggering receptor expressed on myeloid cells-2 (TREM2) for central nervous tissue immune homeostasis. *J Neuroimmunol*. 2007; 184(1–2):92–99. [PubMed: 17239445]
- Paschke M. Phage display systems and their applications. *Appl Microbiol Biotechnol*. 2006; 70(1):2–11. [PubMed: 16365766]
- Ravichandran KS, Lorenz U. Engulfment of apoptotic cells: signals for a good meal. *Nat Rev Immunol*. 2007; 7(12):964–974. [PubMed: 18037898]
- Rothlin CV, Lemke G. TAM receptor signaling and autoimmune disease. *Curr Opin Immunol*. 2010; 22(6):740–746. [PubMed: 21030229]
- Rotshenker S, Reichert F, Gitik M, Haklai R, Elad-Sfadia G, Kloog Y. Galectin-3/MAC-2, Ras and PI3K activate complement receptor-3 and scavenger receptor-AI/II mediated myelin phagocytosis in microglia. *Glia*. 2008; 56(15):1607–1613. [PubMed: 18615637]
- Sano H, Hsu DK, Apgar JR, Yu L, Sharma BB, Kuwabara I, Izui S, Liu FT. Critical role of galectin-3 in phagocytosis by macrophages. *J Clin Invest*. 2003; 112(3):389–397. [PubMed: 12897206]
- Strick DJ, Vollrath D. Focus on molecules: MERTK. *Exp Eye Res*. 2010; 91(6):786–787. [PubMed: 20488176]
- Thorp E, Tabas I. Mechanisms and consequences of efferocytosis in advanced atherosclerosis. *J Leukoc Biol*. 2009; 86(5):1089–1095. [PubMed: 19414539]
- Uehara F, Ohba N, Ozawa M. Isolation and characterization of galectins in the mammalian retina. *Invest Ophthalmol Vis Sci*. 2001; 42(10):2164–2172. [PubMed: 11527926]
- Vlassara H, Li YM, Imani F, Wojciechowicz D, Yang Z, Liu FT, Cerami A. Identification of galectin-3 as a high-affinity binding protein for advanced glycation end products (AGE): a new member of the AGE-receptor complex. *Mol Med*. 1995; 1(6):634–646. [PubMed: 8529130]

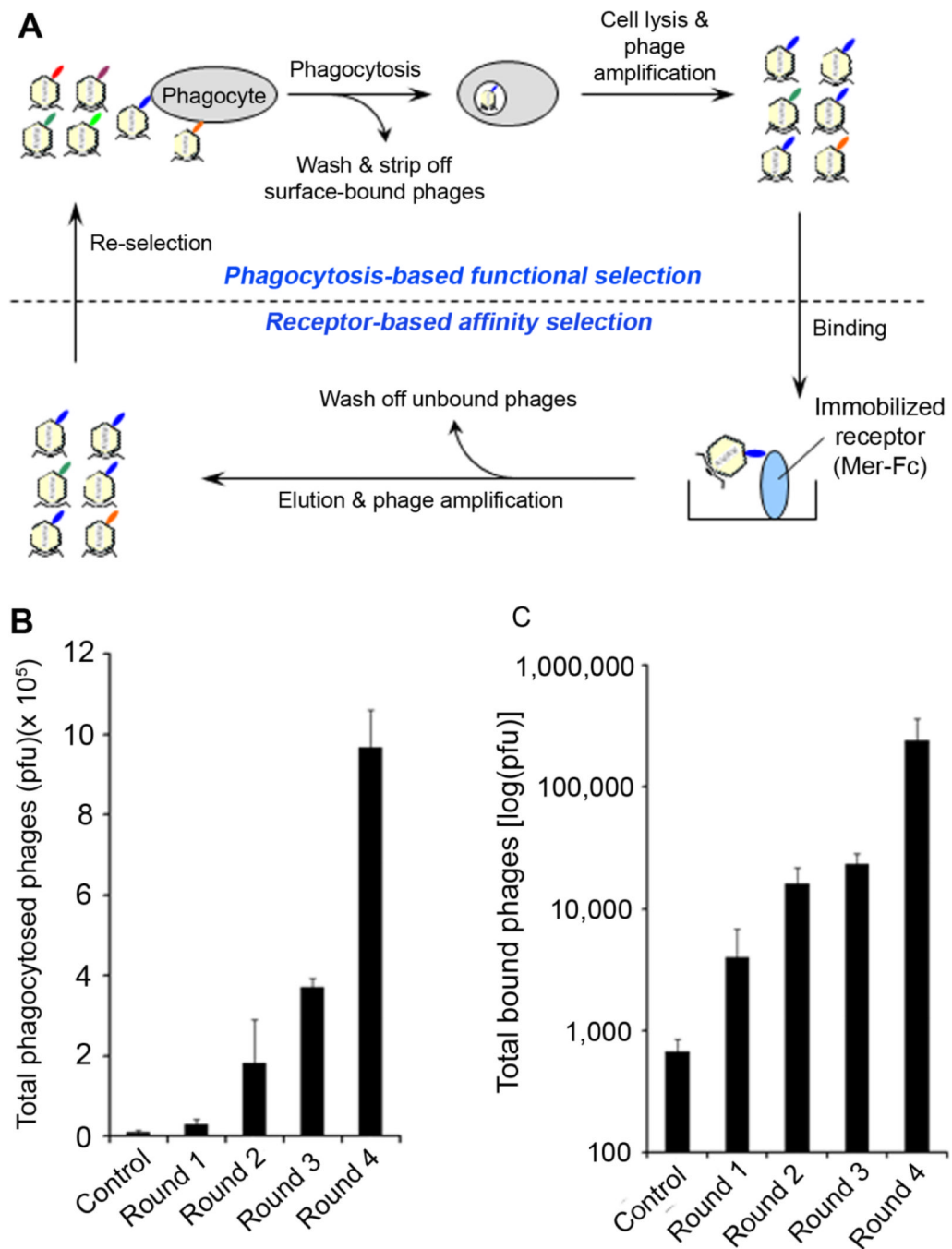


Fig. 1. Dual functional cloning

(A) Phage selection scheme. Dual functional cloning consists of phagocytosis-based functional selection with D407 RPE cells and receptor-based affinity selection with immobilized Mer-Fc. Four rounds of combined selections were performed. (B) Total phages phagocytosed by D407 at each round were quantified by plaque assay. (C) Total phages bound to Mer-Fc at each round were quantified. The control phage was included as a negative control

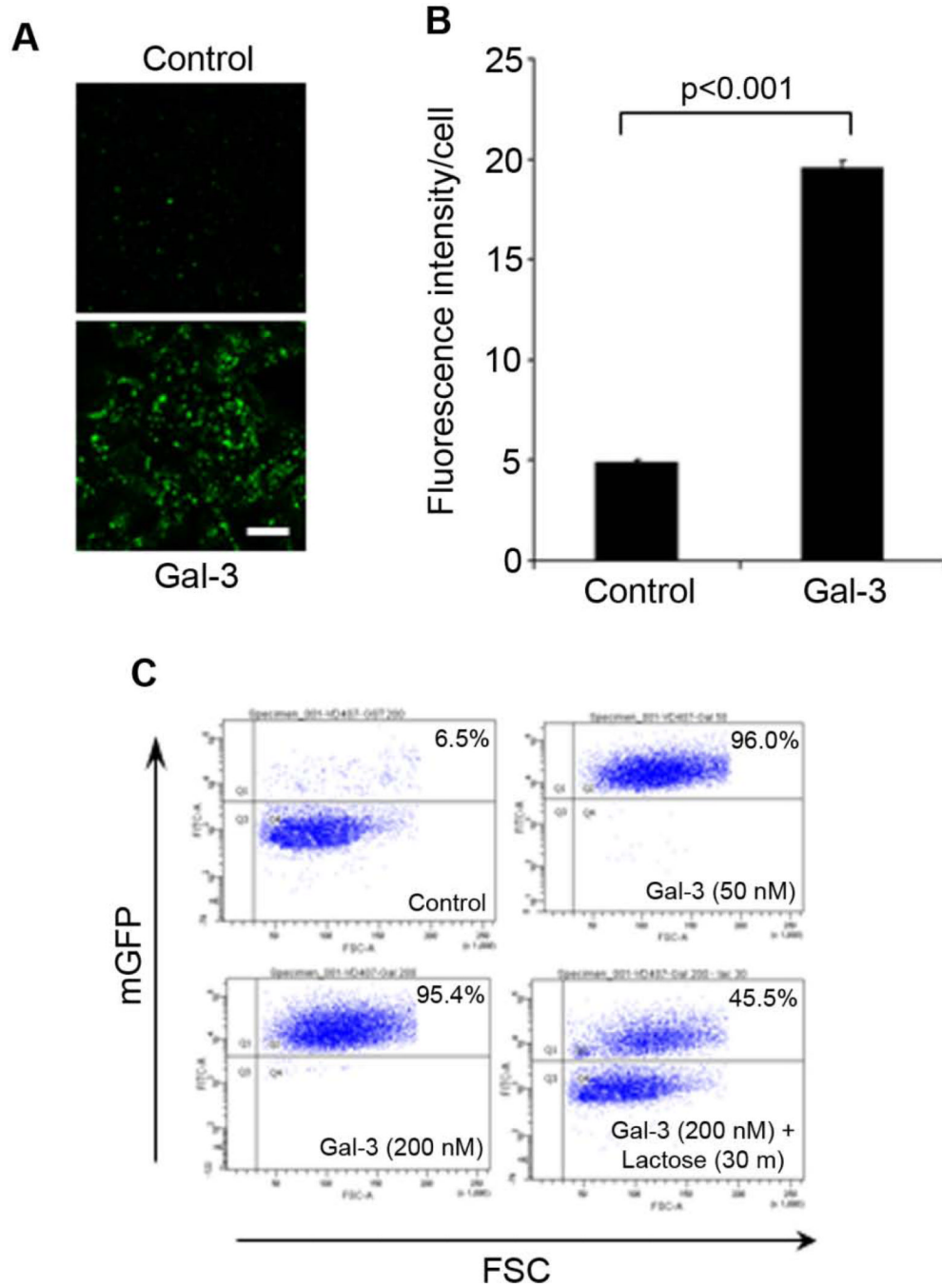


Fig. 2. Gal-3 stimulates RPE phagocytosis

(A) Gal-3 facilitates RPE phagocytosis of membrane vesicles. Gal-3-FLAG was expressed in Neuro-2a cells. mGFP-labeled membrane vesicles were prepared from Gal-3-expressing Neuro-2a cells or control cells and analyzed for RPE phagocytosis in D407 cells. Phagocytosed vesicles were analyzed by confocal microscopy. Multiple z-stack images were analyzed, and only the intracellular z-stacks with the highest DAPI signals were used to analyze the phagocytosed membrane vesicles. However, because DAPI blue signals interfere with the visual perception of GFP signals (Caberoy et al., 2010a), only GFP signals are shown here. Bar = 10 μ m. (B) Relative fluorescence intensity per cells in (A) was

quantified in more than 100 cells per group (\pm s.e.m.; $n > 100$; t-test). (C) Purified Gal-3 stimulates RPE phagocytosis. Control membrane vesicles were prepared from mGFP-expressing Neuro-2a cells and analyzed for RPE phagocytosis in D407 cells in the presence or absence of GST-Gal-3 and lactose. The surface-bound membrane vesicles were removed with trypsin treatment, followed by washing and flow cytometric quantification. FSC; forward scatter (to eliminate surface-bound unphagocytosed cargos).

\$watermark-text

\$watermark-text

\$watermark-text

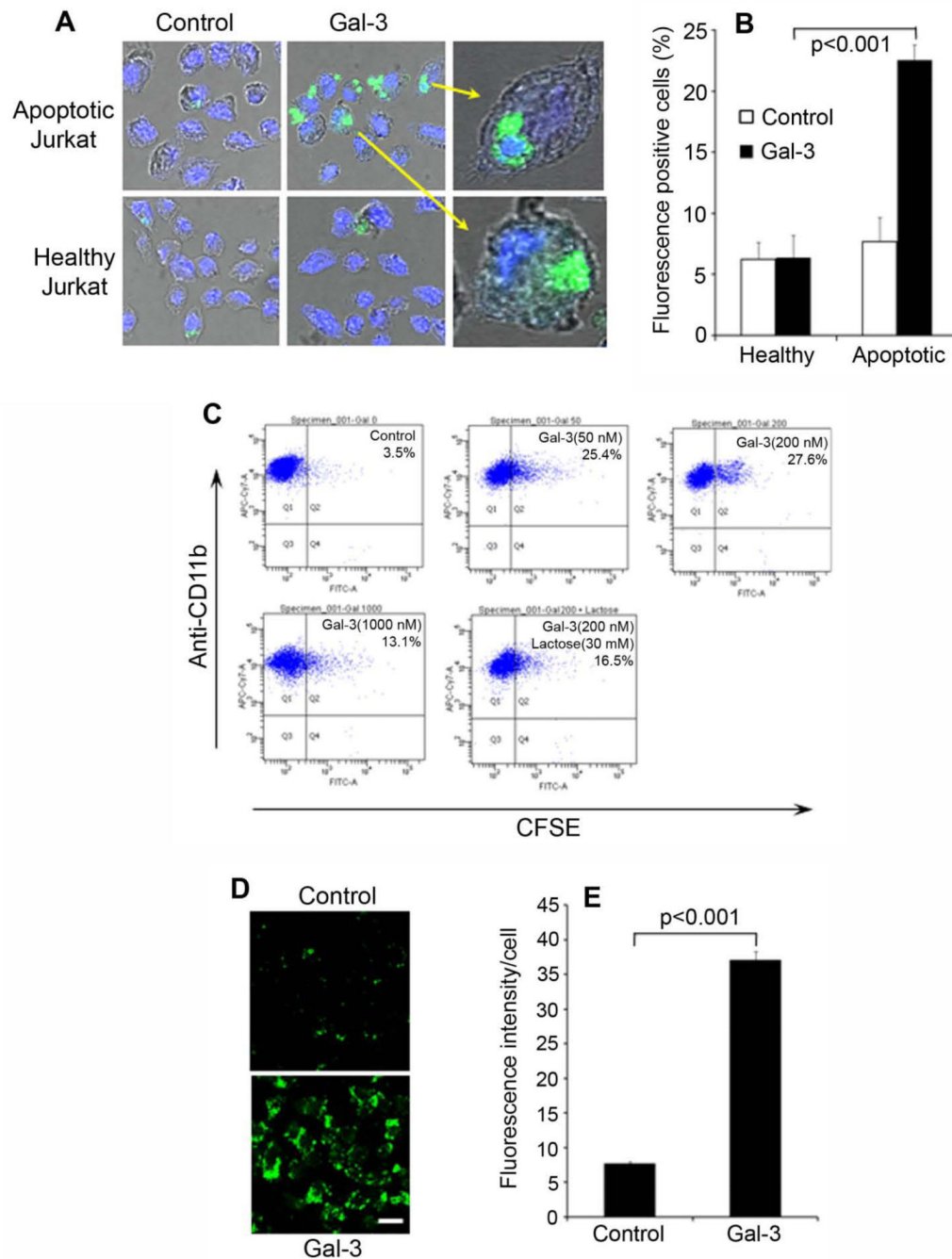


Fig. 3. Gal-3 facilitates macrophage phagocytosis

(A) Gal-3 promotes macrophage phagocytosis of apoptotic cells. Healthy or apoptotic Jurkat cells were labeled with CFSE, washed and incubated with J774 macrophage cells in the presence or absence of Gal-3 (200 nM). The phagocytosis of Jurkat cells was analyzed by confocal microscopy. The intracellular z-stack confocal images of CFSE and DAPI were superimposed with the cognate bright fields to reveal phagocytosed Jurkat cells. (B) Percentage of macrophages with phagocytosed apoptotic cells in (A) were quantified (\pm s.e.m.; $n > 20$; t-test). (C) Macrophage phagocytosis of apoptotic cells in the presence or absence of Gal-3 and lactose was performed as in (A) and analyzed by flow cytometry.

Macrophages were labeled with APC/Cy7-anti-CD11b mAb. **(D)** Gal-3 stimulates macrophage phagocytosis of membrane vesicles. Gal-3-mediated phagocytosis of membrane vesicles by J774 cells was performed, as described in Fig. 2A. **(E)** Relative fluorescence intensity per cell in (D) was quantified in more than 100 cells per group (\pm s.e.m.; $n > 100$; t-test). Bar = 10 μ m.

\$watermark-text

\$watermark-text

\$watermark-text

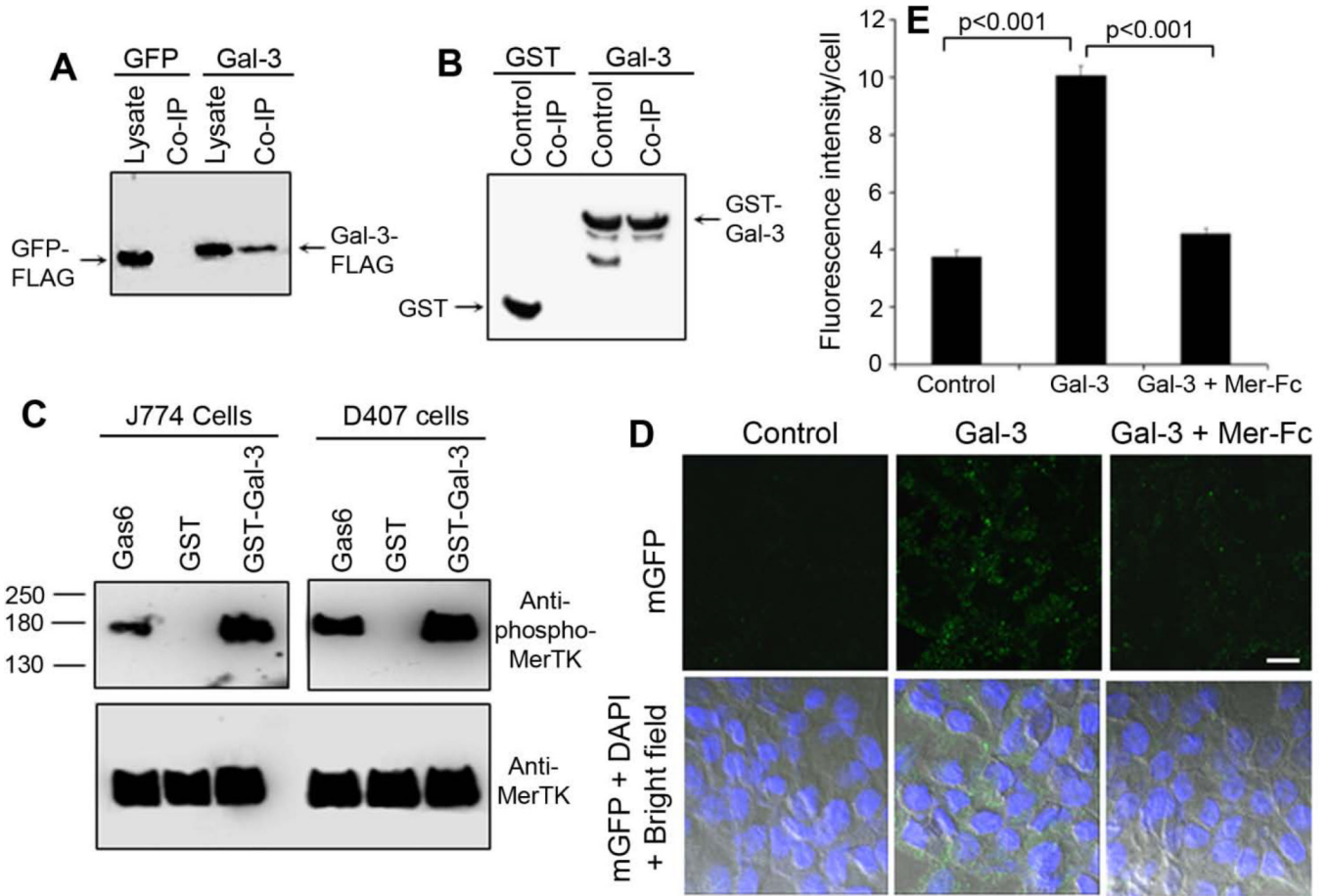


Fig. 4. Gal-3 is a MerTK-specific ligand

(A) Co-immunoprecipitation of Gal-3-FLAG and Mer-Fc. Gal-3-FLAG or GFP-FLAG control was expressed in Neuro-2a cells. Cell lysates were prepared and incubated with Mer-Fc, followed by protein A-agarose beads. After washing, the beads were analyzed by Western blot using anti-FLAG mAb. (B) Co-immunoprecipitation of GST-Gal-3 and Mer-Fc. Purified GST-Gal-3 fusion protein or GST control was incubated with Mer-Fc, co-immunoprecipitated as described above and analyzed by Western blot using anti-GST mAb. (C) Gal-3 activates MerTK with receptor autophosphorylation. J774 and D407 cells were incubated with GST-Gal-3 or GST control (200 nM). MerTK was co-immunoprecipitated and detected by Western blot using anti-phospho-MerTK and anti-MerTK Abs. Gas6 (50 nM) was included as a positive control. (D) mGFP-labeled Neuro-2a membrane vesicles were incubated with purified GST-Gal-3 (200 nM), washed to remove unbound Gal-3 and analyzed for RPE phagocytosis in the presence or absence of excessive Mer-Fc (1 µg/ml). Gal-3 was capable of associating with the membrane vesicles and stimulating RPE phagocytosis. Mer-Fc blocked Gal-3 stimulation of RPE phagocytosis. Bar = 10 µm. (E) Relative fluorescence intensity per cells in (D) was quantified in more than 100 cells per group (± s.e.m.; n>100; t-test).